First-principles calculations of electronic and optical properties of $Fe_{3-x}V_xAl$ (x = 0–3) compounds

2009 J. Phys.: Condens. Matter 21 446001

(http://iopscience.iop.org/0953-8984/21/44/446001)

J. Phys.: Condens. Matter **21** (2009) 446001 (10pp) doi:10.1088/0953-8984/21/44/446001

First-principles calculations of electronic and optical properties of $Fe_{3-x}V_xAl$ ($x = 0$–3) compounds

Manish Kumar[1,2], **Tashi Nautiyal**[1] **and Sushil Auluck**[3]

[1] Department of Physics, Indian Institute of Technology Roorkee, Roorkee 247667, Uttarakhand, India
[2] Department of Physics, Kurukshetra University, Kurukshetra 136119, Haryana, India
[3] Department of Physics, Indian Institute of Technology Kanpur, Kanpur 208016, Uttar Pradesh, India

E-mail: manishdft@gmail.com

Received 15 May 2009, in final form 7 September 2009
Published 9 October 2009
Online at stacks.iop.org/JPhysCM/21/446001

Abstract

We present calculations of the electronic and optical properties for $Fe_{3-x}V_xAl$ ($x = 0$–3) compounds with the aim of studying the effect of increasing the concentration of vanadium. We also report calculations of the magneto-optical (MO) Kerr effect, which depends on the off-diagonal components of the optical conductivity (OC), for the magnetic compounds Fe_3Al and V_2FeAl. This systematic analysis of the electronic structure and optical properties of $Fe_{3-x}V_xAl$ compounds has been carried out using the full potential linearized augmented plane wave (FPLAPW) method within the generalized gradient approximation (GGA). The results, presented at equilibrium lattice constant, show that the compounds Fe_3Al, V_2FeAl and V_3Al are metallic whereas the Fermi level lies at the 'pseudogap' in Fe_2VAl. The OC spectra exhibit one main peak around 2.5 eV for all the compounds. The calculated OC spectra for Fe_2VAl and Fe_3Al shows the same features as in the experimental spectra, resulting a good qualitative agreement: however, the magnitude is overestimated. The blueshifting of structures in Fe_2VAl is discussed. Our results show that the two compounds exhibit a contrast in terms of intraband transitions which help to achieve a good agreement with experiment in Fe_3Al and remain at low key in Fe_2VAl. The peaks in the optical conductivity can be explained as arising out of the transitions from Al p to Fe 3d and/or V 3d in these compounds. The calculations for MO spectra of the compounds Fe_3Al and V_2FeAl show small Kerr rotations.

(Some figures in this article are in colour only in the electronic version)

1. Introduction

Heusler-type ternary and pseudobinary compounds X_2YZ (where X and Y denote the metal atoms and Z is a metalloid) in the $L2_1$ and DO_3 structures display a remarkably rich variety of behavior in their electronic, magnetic and transport properties. A detailed report about the electrical and magnetic properties of $Fe_{3-x}V_xAl$ compounds with vanadium concentration $x = 0$–1.15 has been presented by Kato *et al* [1]. Their results clearly demonstrate that the compounds are ferromagnetic, at least in the concentration range of $x = 0$–0.9. They found that the Curie temperature T_c decreases with an increase in the vanadium content and the magnetic moment of iron decreases more abruptly than in the simple iron–vanadium solid solution. Also that, with an increase in x, regions with a negative temperature coefficient appear in the resistivity versus temperature curves. For compounds with $x = 1$ (i.e. Fe_2VAl) and 1.15, a semiconductor-like behavior was observed in the whole temperature range of 2–1200 K. The magnitude of the semiconductor bandgap was found to be 0.10 eV for Fe_2VAl as determined from the linearization of $\ln\rho = f(1/T)$ dependence in the temperature range 400–800 K [1]. According to experimental data on the nuclear magnetic resonance [2] and temperature-dependent resistivity [1], the

ground state of the Heusler phase Fe_2VAl ($L2_1$ structure) was classified as a narrow-gap semiconductor. First-principles calculations of the energy band spectrum for Fe_2VAl carried out within the density functional theory [3–5] show that this compound is a nonmagnetic semimetal with a narrow 'pseudogap' at the Fermi level (E_F) due to hybridization effects. Later Bansil *et al* [6] investigated the evolution of the electronic structure in the $Fe_{3-x}V_xAl$ ($x = 0$, 0.25, 0.5, 0.75, 1) system using the Korringa–Kohn–Rostoker method with coherent-potential approximation (KKR–CPA) and noted a drastic change in the partial density of states at the Fermi level with an increase in vanadium content which results in the formation of a 'pseudogap' at the Fermi level in the compounds rich in vanadium.

The compound Fe_3Al ($x = 0$) has a number of unusual electronic and magnetic properties that makes it attractive for high temperature applications. It is ferromagnetic with T_c as 713 K [7]. It has two types of Fe atoms: Fe^I and Fe^{II} (as discussed later). Neutron diffraction measurements [8] yield local magnetic moments as 1.50 μ_B for Fe^I, 2.18 μ_B for Fe^{II} and zero for Al in this compound. Thus, as expected from the same nearest-neighbor environments for Fe^{II} as in elemental bcc Fe, the magnetic moment for Fe^{II} (2.18 μ_B) is very close to that of elemental bcc Fe (2.21 μ_B) [9]. In recent years, there has been considerable interest in the electronic and optical properties of Fe_3Al and Fe_2VAl. Okamura *et al* [10] measured their near-normal incidence reflectivity by using a Fourier interferometer. The optical conductivity spectra were obtained from reflectivity measurements using the Kramers–Kronig relations [11]. This confirmed the existence of a 'pseudogap' at E_F in Fe_2VAl. The optical conductivity spectra for $Fe_{3-x}V_xAl$ compounds ($x = 0$–1.1) at room temperature have been investigated by Shreder *et al* [12] from resistivity $\rho(T)$ measurements.

The other two compounds of this series are V_2FeAl and V_3Al for $x = 2$ and 3, respectively. V_3Al has been reported [13] to occur in the cubic A15 (Cr_3Si) structure (also known as the β–W structure). Watson and Weinert [14] have studied these compounds using the full potential linearized augmented Slater-type orbital (FPLASTO) method within the local density approximation (LDA). The stability of the $L2_1$ and A15 structures for V_2FeAl and V_3Al, respectively, was analyzed on the basis of their heat of formation. V_2FeAl was found to be ferrimagnetic and V_3Al to be nonmagnetic [14]. However, there appears to be no experimental study on the Heusler compound V_2FeAl. Hence these four compounds (Fe_3Al, Fe_2VAl, V_2FeAl and V_3Al) make an interesting group with different kinds of crystal structures and properties. To develop a better understanding of the behavior of these $Fe_{3-x}V_xAl$ compounds and to understand the effect of increasing vanadium concentration for the composition range $0 \leqslant x \leqslant 3$ (integral values), we have performed first-principles calculations of electronic and magnetic properties of these compounds. Since density functional theory (DFT) focuses on the ground state, therefore the true check on the electronic structure calculations is to test these for the excited state properties, like optical and magneto-optical properties, also. The optical properties of these compounds are helpful to describe the interaction of light and to gain insight about how it is affected on varying the concentration of V. Moreover, the MO properties are useful in recording technology and Kerr spectroscopy. Furthermore, we are not aware of any calculations for the optical conductivity of these compounds even though experimental data is there for Fe_3Al and Fe_2VAl. Hence, besides studying the ground state properties, we also calculated the optical properties of these compounds. In fact, we have offered a more stringent test for our band structure calculations by calculating the magneto-optical Kerr angle and ellipticity which depend on the small off-diagonal components of the optical conductivity. Experimental measurements on the same are awaited and would be welcome to check the degree of accuracy of our calculated results. This paper is organized as follows. The theory underlying the optical and magneto-optical properties is briefly outlined in section 2. Crystal structure of $Fe_{3-x}V_xAl$ compounds and computational details are presented in section 3. The results are presented and compared with available experimental and theoretical results in section 4. Finally the conclusions are drawn in section 5.

2. Theory

We have adopted the dipole approximation in calculations of optical properties, i.e. the momentum transfer from the initial state to the final state was neglected by considering vertical transitions. With some approximations, the Kubo formula [15, 16] for the optical conductivity tensor is written in the form

$$\sigma_{\alpha\beta}(\omega) = \frac{Ve^2}{8\pi^2\hbar m^2\omega}\sum_{nn'}\int \mathrm{d}^3k\langle kn|p_\alpha|kn'\rangle \times \langle kn|p_\beta|kn'\rangle f_{kn}(1-f_{kn'})\delta(E_{kn'}-E_{kn}-\hbar\omega) \quad (1)$$

where $\alpha, \beta = 1, 2, 3$; p_α are components of the momentum operator, f_{kn} is the Fermi distribution function ensuring that only transitions from occupied to unoccupied states are considered and $|kn\rangle$ is the crystal wavefunction corresponding to the Kohn–Sham eigenvalue E_{kn} with crystal momentum (k). Equation (1) containing a double sum over all energy bands naturally splits into the interband ($n \neq n'$) and intraband ($n = n'$) contributions, i.e.

$$\sigma_{\alpha\beta}(\omega) = \sigma_{\alpha\beta}^{\mathrm{inter}}(\omega) + \sigma_{\alpha\beta}^{\mathrm{intra}}(\omega). \quad (2)$$

For the diagonal tensor components, both the terms are important and should be considered simultaneously. The intraband contribution, meaningful only for metals (or half-metals), is usually described by the phenomenological expression according to the Drude–Sommerfeld model [17, 18] as

$$\sigma_D(\omega) = \frac{\omega_p^2}{4\pi\left[\frac{1}{\tau_1} - i\omega\right]}, \quad (3)$$

where ω_p is the plasma frequency and τ_1 is the intraband relaxation time which characterizes the scattering of charge carriers.

The imaginary part of the off-diagonal elements of the conductivity tensor describes the magneto-optical absorption. This absorptive part is directly proportional to the difference

between the absorption of left (−) and right (+) circularly polarized light and its sign is directly related to the spin polarization of the states responsible for interband transitions. The refractive indices $n_\pm$ for circularly polarized waves, are directly related to the dielectric tensor or conductivity tensor as given by

$$n_\pm^2 = \varepsilon_{xx} \pm \mathrm{i}\varepsilon_{xy} = 1 + \frac{4\pi\,\mathrm{i}}{\omega}(\sigma_{xx} \pm \mathrm{i}\sigma_{xy}). \tag{4}$$

The expression for small values of Kerr angle can be simplified to [19]

$$\theta_k + \mathrm{i}\varepsilon_k = \frac{-\sigma_{xy}}{\sigma_{xx}\sqrt{1 + \frac{4\pi\mathrm{i}}{\omega}\sigma_{xx}}}. \tag{5}$$

A detailed theory of magneto-optics can be found in [20].

3. Calculational and structural details

First-principles total energy calculations of $Fe_{3-x}V_xAl$ (x = 0–3) compounds were carried out using the WIEN2k [21] implementation of the full potential linearized augmented plane wave (FPLAPW) method [22] based on the DFT [23, 24]. We used the generalized gradient approximation (GGA) [25] for the electronic exchange and correlation according to Perdew–Burke–Ernzerhof parameterization [26]. The potential and the charge in the crystal are treated with no shape approximation. The radii of muffin tin spheres were chosen as $R_{\mathrm{MT}}^{\mathrm{V}} = R_{\mathrm{MT}}^{\mathrm{Fe}} = 2.1$ au and $R_{\mathrm{MT}}^{\mathrm{Al}} = 2.3$ au The cutoff parameters were decided by $R_{\mathrm{MT}}K_{\mathrm{Max}} = 9$ for the plane waves and $G_{\mathrm{Max}} = 14$ au^{-1} was used in the Fourier expansion of the potential in the interstitial region. The k-space integration has been done by the modified tetrahedron method [27]. We have checked the convergence of the calculated eigenvalues with respect to the number of augmented plane waves and also with respect to the number of k-points used. Self-consistency has been obtained using 195 k-points in the irreducible Brillouin zone (IBZ). To calculate the optical properties, a dense mesh of 726 k-points in the IBZ has been used. The spin–orbit interaction is taken into account in the second variation in each self-consistency loop [28] for the compounds Fe_3Al and V_2FeAl as both are found to be magnetic.

The Heusler compounds Fe_2VAl and V_2FeAl have cubic $L2_1$ structure such that there are 16 atoms in the unit cell. This is a close packed complex cubic structure which is formed by four interpenetrating fcc sublattices. In Fe_2VAl, the Fe atoms occupy 8c Wyckoff positions (1/4 1/4 1/4), the Al atoms occupy the 4a positions (0 0 0) and the V atoms are placed at 4b sites (1/2 1/2 1/2). All atoms have eight nearest neighbors. The V and Al atoms have eight Fe atoms as the nearest neighbors while for Fe there are four V and four Al atoms. In the same manner, one can make out the atomic positions in the compound V_2FeAl.

When V is replaced by Fe in Fe_2VAl, one gets an intermetallic compound Fe_3Al with the DO_3 crystal structure. There are three Fe atoms per unit cell in Fe_3Al which are distributed among two non-equivalent sites named as Fe^{I} (two atoms) and Fe^{II} (one atom) with specific neighbor configurations. The former (Fe^{I}) has four Al and four Fe^{II} atoms as nearest neighbors in a tetrahedral coordination while the latter (Fe^{II}) is surrounded by eight iron (Fe^{I}) atoms offering a bcc environment. Here it is important to note that the Fe^{I} site is quite different from the Fe^{II} site, not only in terms of coordination but also in size. In particular, Fe^{II} is larger in size and has no Al neighbors. The Fe^{I} atoms are present at (1/4 1/4 1/4) and (3/4 3/4 3/4) and Fe^{II} at (1/2 1/2 1/2) in the unit cell. The Al atom occupies the (0 0 0) position. All the atoms in the fcc DO_3 and ordered $L2_1$ crystal structure align on the high symmetry axis (space group $Fm3m$). Accordingly, the only free crystallographic parameter is the lattice constant. The compound V_3Al, richest in V in this series with $x = 3$ in $Fe_{3-x}V_xAl$, exists in an A15 structure with $pm3n$ space group. Its unit cell contains two Al and six V atoms which are present at equivalent positions (0 0 0) and (1/4 0 1/2), respectively.

4. Results and discussions

From the previous works, we know that Fe_2VAl [14, 29, 30] and V_3Al [13, 31] are nonmagnetic (NM) whereas Fe_3Al [7, 14, 30] is ferromagnetic. Hence for these compounds, we have performed the structural optimization in their respective nonmagnetic/magnetic state in the neighborhood of their experimental lattice constant. The Heusler compound V_2FeAl has not been reported yet experimentally; hence we term it as a 'hypothetical' compound and explored nonmagnetic, ferromagnetic and ferrimagnetic states for this. The structural optimization for this compound yields the total energy minimum in the same range of lattice parameters as for Fe_3Al and Fe_2VAl. The optimized lattice parameters for all the compounds are defined by the total energy minimum in the optimization plot as shown in figure 1 and the equilibrium values of lattice parameter a are summarized in table 1. The experimental values of the lattice constants [13, 32] and of the available magnetic moments [7, 8, 34] are also listed in the table. The calculated equilibrium lattice parameters for Fe_3Al and Fe_2VAl compounds are found to be within 1%, on average, of the available experimental lattice parameters [32] and within 2.5% for V_3Al [13]. Our results for these compounds have also been compared with previous calculations [14, 29, 33, 35]. Our calculations show V_2FeAl to be ferrimagnetic, which is consistent with the calculations of Watson and Weinert [14]. The ferrimagnetic state is found to be more stable as compared to the ferromagnetic state (by a small margin of 0.016 eV/f.u.) and nonmagnetic state (by a fair margin of 0.25 eV/f.u.).

The site-resolved magnetic moments for V_2FeAl and Fe_3Al are also listed in table 1. The total magnetic moment for Fe_3Al (5.96 μ_B) is very high. Though it exceeds the experimental value (5.61 μ_B) it shows better agreement compared to previous calculations. The overestimation is mainly due to the larger magnetic moment assigned to Fe sites in comparison to the experiment. It is worth mentioning here that the site-resolved magnetic moments from Watson and Weinert [14] seem to be closer to their experimental counterparts. However, it may be noted that their values are calculated at a lattice constant (5.602 Å) smaller than the experimental or the equilibrium lattice constant. To compare our results vis à vis theirs, we also calculated the magnetic

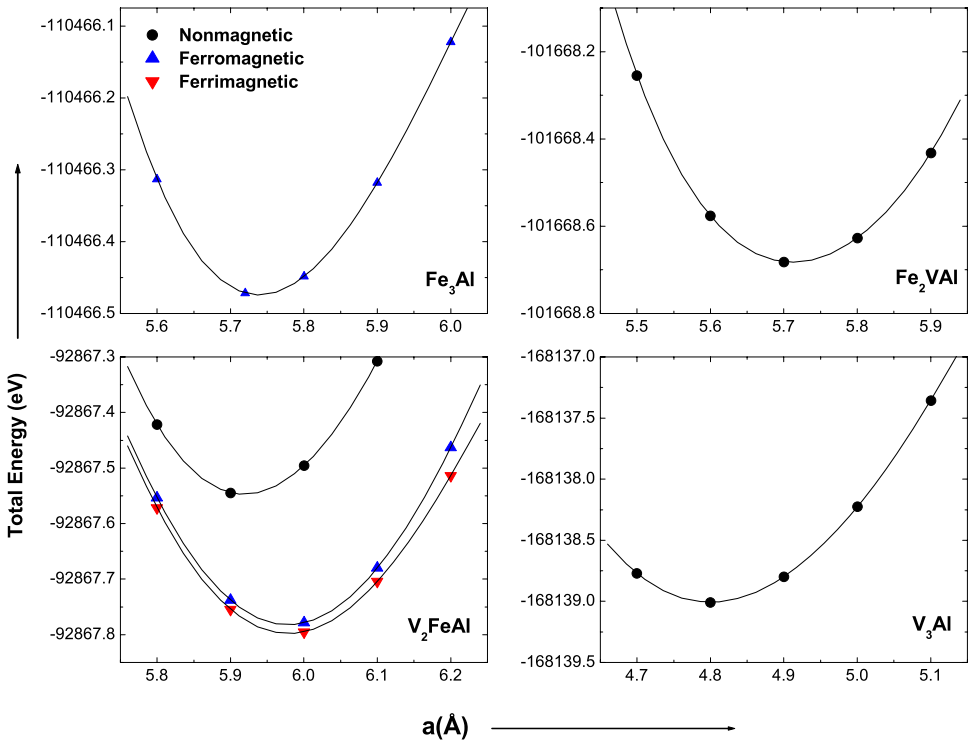

Figure 1. Total energy versus lattice parameter for $Fe_{3-x}V_xAl$ ($x = 0$–3) compounds. The solid lines show a polynomial fit for determining the equilibrium lattice constants.

Table 1. The optimized lattice parameters a (Å), $\Delta a/a$ (the % change in lattice parameters w.r.t. experimental value), partial and total magnetic moments (μ_B) for FM Fe_3Al and V_2FeAl. Total DOS at Fermi level $N(E_F)$ (states/eV/cell) and coefficient of specific heat γ (in mJ mol^{-1} K^{-2}) for $Fe_{3-x}V_xAl$ ($x = 0$–3) compounds.

					μ						
x	$Fe_{3-x}V_xAl$	Reference	a (Å)	$\Delta a/a$	Fe^I	Fe^{II}	V	Al	Total	$N(E_F)$	γ
0	Fe_3Al	This work	5.742	0.83	1.92	2.40	—	−0.10	5.96	2.84	6.68
		Theory[a]	5.761	0.50	1.96	2.51	—	−0.12	6.10	2.78	6.54
		[b]	—	—	1.89	2.34	—	−0.14	—	—	—
		[c]	—	—	1.90	2.44	—	−0.10	6.03	—	—
		[d]	5.602	3.25	1.59	2.21	—	—	—	—	—
		Expt	5.79[e]	—	1.45[f]	2.20[f]	—	—	5.61[g]	—	—
			—	—	1.5[h]	2.18[h]	—	0.0[h]	—	3.09[a]	7.27[a]
1	Fe_2VAl	This work	5.712	0.83	—	—	—	—	—	0.19	0.45
		Theory[a]	5.712	0.83	—	—	—	—	—	0.18	0.42
		[d]	5.594	2.88	—	—	—	—	—	—	—
		Expt	5.76[e]	—	—	—	—	—	—	0.18[i]	0.42[i]
2	V_2FeAl	This work	5.978	—	—	1.91	−0.57	0.00	0.46	6.62	15.57
		Theory[d]	5.839	—	—	1.15	−0.19	—	—	—	—
3	V_3Al	This work	4.81	2.24	—	—	—	—	—	19.3	45.4
		Theory[d]	4.75	3.45	—	—	—	—	—	—	—
		Expt[j]	4.92	—	—	—	—	—	—	—	—

[a] Reference [29]. [b] Reference [33]. [c] Reference [35]. [d] Reference [14]. [e] Reference [32].
[f] Reference [7]. [g] Reference [34]. [h] Reference [8]. [i] Reference [36]. [j] Reference [13].

moment at this smaller value of 5.602 Å and found that the magnetic moment values for Fe^I and Fe^{II} come out to be 1.63 μ_B and 2.26 μ_B, respectively, which are very close to those reported in [14] (1.59 and 2.21 μ_B, respectively), and also to the experimental values (1.5 and 2.18 μ_B, respectively). The magnetic moment on the Al atom is negligible but is oppositely directed, from all the calculations, to that at Fe sites, thereby lowering the total magnetic moment. Thus its magnetic property is coupled strongly to the crystalline structure. To estimate the closeness in the environment of the Fe^{II} sites in Fe_3Al to that in pure elemental Fe, we calculated the nearest-neighbor (n-n) distances for each of the cases. Interestingly, the Fe^I–Fe^{II} distance (2.48 Å) in Fe_3Al is very close to the Fe–Fe distance (2.47 Å) in pure Fe. There are 8 Fe^I nearest neighbors

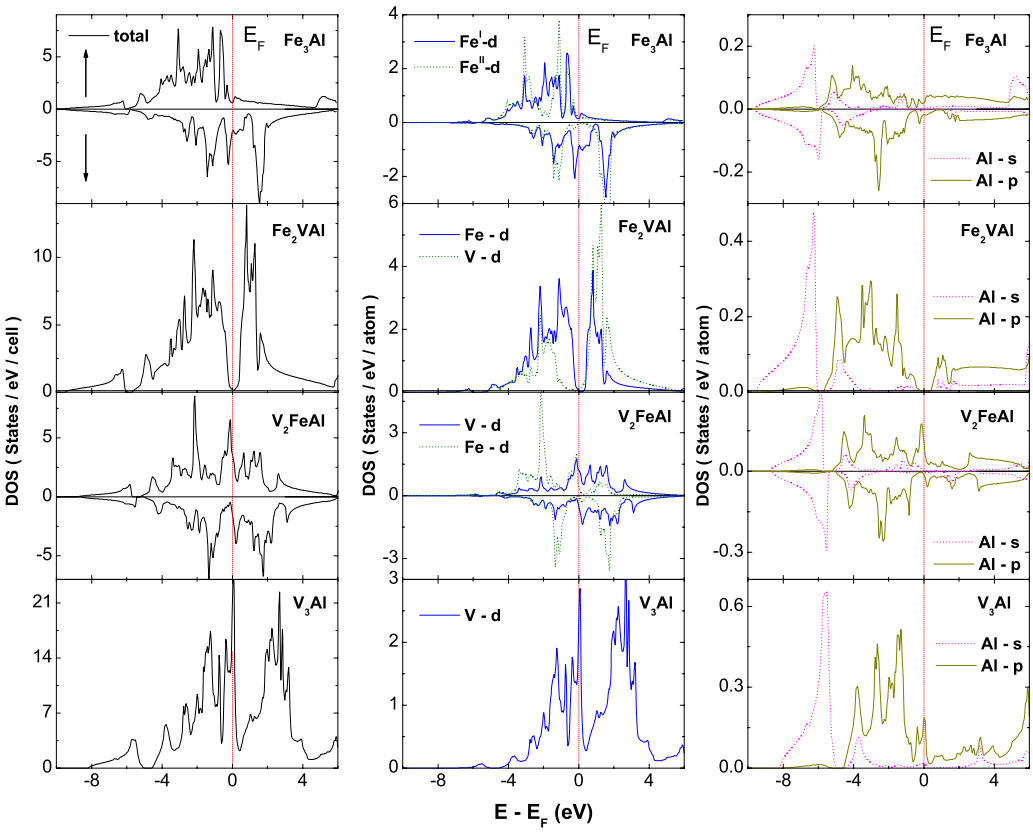

Figure 2. Total and spin projected density of states (DOS) of $Fe_{3-x}V_xAl$ ($x = 0$–3) compounds. E_F represents the Fermi level.

Table 2. Environment at the two inequivalent Fe sites (Fe^I and Fe^{II}) in Fe_3Al.

Fe^I at (1/4 1/4 1/4)	Fe^{II} at (1/2 1/2 1/2)
First nearest neighbors: (8; bcc environment) 4 Fe^{II} at (1/2 0 0), (0 1/2 0), (0 0 1/2) and (1/2 1/2 1/2) 4 Al at (0 0 0), (1/2 1/2 0), (1/2 0 1/2) and (0 1/2 1/2)	*First nearest neighbors:* (8; bcc environment) 8 Fe^I at (3/4 1/4 1/4), (1/4 3/4 1/4), (1/4 1/4 3/4), (1/4 1/4 1/4), (3/4 3/4 3/4), (3/4 3/4 1/4), (3/4 1/4 3/4) and (1/4 3/4 3/4)
Second nearest neighbors: (6; sc arrangement as in bcc environment) 6 Fe^I at (1/4 1/4 −1/4), (1/4 −1/4 1/4), (3/4 1/4 1/4), (−1/4 1/4 1/4), (1/4 3/4 1/4) and (1/4 1/4 3/4)	*Second nearest neighbors:* (6; sc arrangement as in bcc environment) 6 Al at (1/2 1/2 0), (1/2 0 1/2), (1 1/2 1/2), (0 1/2 1/2), (1/2 1 1/2) and (1/2 1/2 1)

to each Fe^{II} atom as in bcc Fe (see table 2). Due to this, we obtain approximately the same magnetic moment for Fe^{II} in Fe_3Al as for elemental Fe. This shows that the n-n interactions constitute the major part of the exchange field or Weiss field responsible for the ferromagnetism in Fe.

Both inequivalent Fe atoms have significant magnetic moment in Fe_3Al (or Fe_2FeAl) whereas in V_2FeAl, the magnetic moment on the V site is relatively lower and also it is directed antiparallel to that of Fe which leads to a smaller total magnetic moment (0.46 μ_B) for this compound. However, it is noteworthy that pure V is nonmagnetic, therefore the magnetic moment on V in V_2FeAl is having an induced character. Our calculations predict ferrimagnetic ordering for this compound with almost zero magnetic moment induced on the Al site whereas we have small but finite magnetic moment on Al in Fe_3Al. The prediction of ferrimagnetic ordering in V_2FeAl is in agreement with the FPLASTO–LDA calculations from Watson and Weinert [14] which yield relatively smaller magnetic moments at Fe and V sites as compared to ours. This difference may be attributed to their having used a lattice constant smaller than ours by 2.3%. Our results are expected to be quite accurate as we have used GGA, which is known to work better than LDA for Heusler compounds [37] and for transition metals, in general [38]. Experimental results on V_2FeAl are welcome to confirm the magnetic moment values.

The total (for NM cases) and spin polarized (for magnetic cases) density of states (DOS) of these $Fe_{3-x}V_xAl$ compounds is shown in figure 2. The majority states in Fe_3Al are almost full whereas minority states are only partly occupied leading to a sizable magnetic moment for this compound. At E_F,

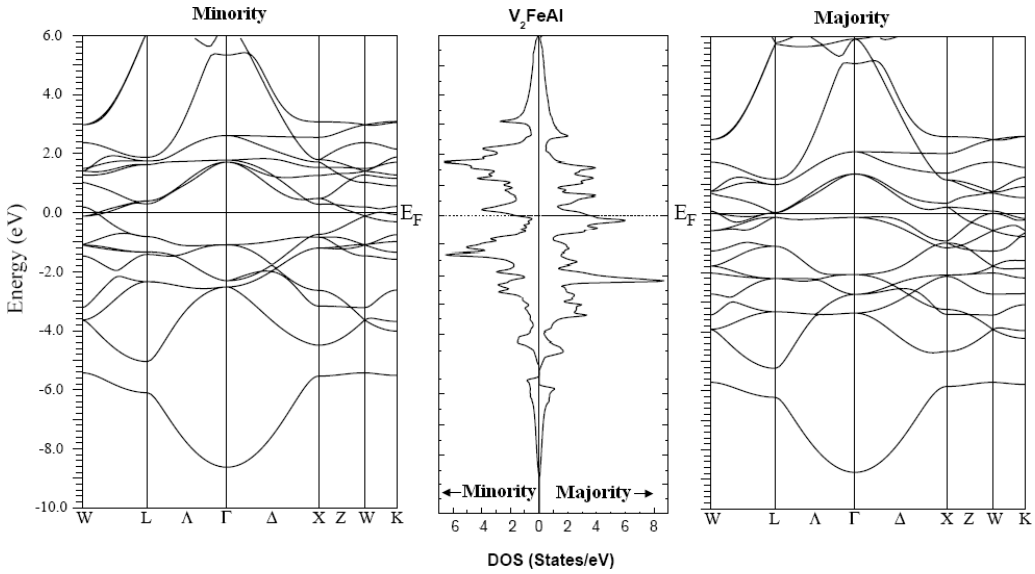

Figure 3. Band structure and DOS of V_2FeAl for minority (left) and majority (right) states.

the major contribution is from Fe^{I} 3d states. The conduction band contains mainly the minority spin states from both the inequivalent Fe atoms in this compound. For the nonmagnetic Fe_2VAl compound, there is a deep minimum in the DOS precisely where the Fermi level (E_F) falls. Hence E_F is situated at the dip, i.e. at the region where there is a negligible DOS. In other words, the valence and conduction bands (VB and CB, respectively) are separated by a 'pseudogap'. The DOS, however, does not vanish here due to a very small overlap of a V-derived conduction band minimum with valence band maximum arising from Fe-derived holes (recall that in this compound both the Fe atoms are equivalent). The partial DOS indicates that the valence band mainly consists of Fe 3d states and the conduction band has both V 3d and Fe 3d states, particularly near E_F. The V atom, which is in the bcc environment, displays two peaks in DOS separated by a region of low density due to the crystal field. However, the exchange splitting is zero and the magnetic ordering does not materialize in the compound Fe_2VAl.

The next compound V_2FeAl contains V and Fe atoms at X and Y positions, respectively, in the unit cell of the X_2YZ Heusler compound. As already mentioned, the Y site offers a bcc environment and is occupied by Fe, while the minority spin states of the Fe atom are largely unoccupied. Thus a sizable magnetic moment (1.91 μ_B) is induced at the Fe site. Due to hybridization of V 3d and Fe 3d states, a magnetic moment of 0.57 μ_B appears at the V site which is antiparallel to that at the Fe site. The last compound of the series, V_3Al, crystallizing in the A15 structure contains only one type of V atom as compared to DO_3 structured Fe_3Al which contains Fe^{I} and Fe^{II} atoms. Due to the presence of nonmagnetic constituents V and Al and there being no favorable factors for the onset of magnetism, this compound remains nonmagnetic. The site-resolved DOS shows that the major contribution to the total DOS comes from V d states in this compound. The partial DOS of Al 3s and Al 3p states are very low for all the present compounds (note the y scales in figure 2) and contribute negligibly to the overall DOS.

Our calculations yield the band structures for Fe_3Al and Fe_2VAl compounds that are in good agreement with those reported by Xu *et al* [30] using FPLAPW calculations within GGA. Therefore we present, at equilibrium lattice constant, the band structures of the remaining two compounds V_2FeAl and V_3Al only. In figure 3, the spin polarized DOS and band structure of ferrimagnetic V_2FeAl are shown. The DOS at E_F has Fe 3d and V 3d characters. The band structures of the majority and the minority spin states indicate that V_2FeAl is metallic due to the presence of overlapping bands in the vicinity of E_F. The lowest valence band (from -8.6 to -5.6 eV for both the majority and minority spin states) is almost entirely due to Al 3s electronic states. The upper dispersed bands have arisen due to the hybridization of V 3d and Fe 3d states with smaller contribution from Al 3p states in the occupied region. The conduction band contains mainly the V 3d and Fe 3d states. Both the minority and majority states contribute to the conduction band in V_2FeAl whereas in Fe_3Al, minority states have overwhelming dominance.

For V_3Al (the A15 structured nonmagnetic compound), the total DOS and band structure are presented in figure 4. Here the V atom is nonmagnetic individually. But unlike the case of Fe_2VAl, no 'pseudogap' is observed at E_F and there is a finite DOS at the E_F. The unit cell of V_3Al contains 2 f.u. Since each V atom has a total of five valence electrons in the 3d and 4s orbitals, we expect 30 electrons/unit cell in the corresponding energy band states. Similarly each Al atom contains two 3s electrons and one 3p electron, making it a total of six electrons from the two Al atoms per unit cell. This yields a total of 36 electrons/unit cell for V_3Al. As a consequence, there are a good number of bands. Assuming each band is doubly occupied by electrons of either spin, the Fermi level must fall somewhere in the vicinity of the 18th band. Our calculations show that six bands (band indices 15th to 20th, disregarding the core states) intersect the Fermi level. As a result, there is a

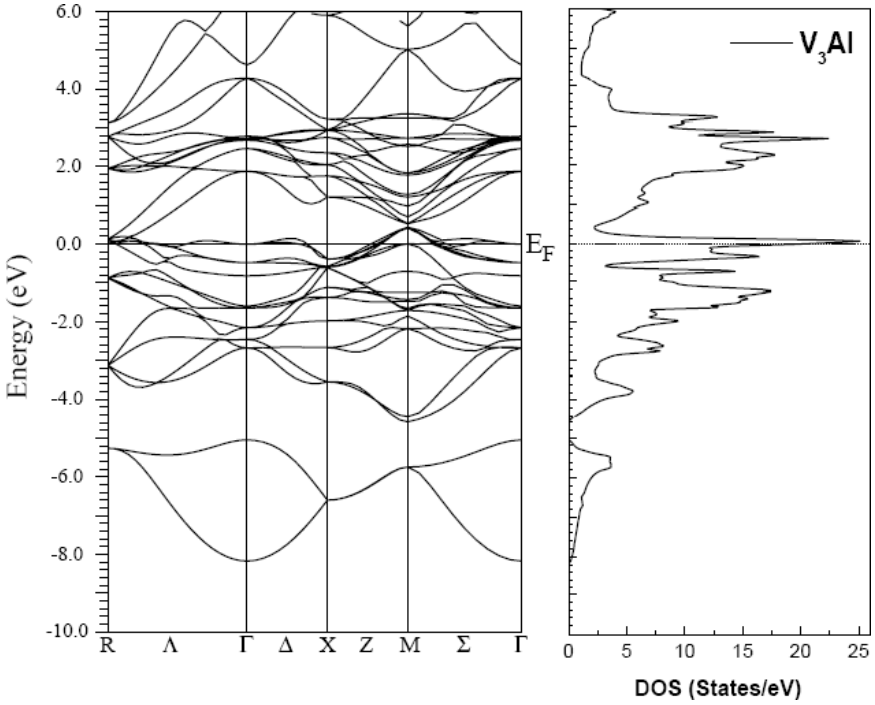

Figure 4. Band structure and DOS of V_3Al.

fairly large DOS at E_F. The deep lying Al 3s states are hardly affected by the environment and appear as a 3 eV wide split-off band from −8.2 to −5.2 eV in this compound, as also in others. The remainder of the valence band manifold, which extends from −4.4 eV to E_F may be regarded as V 3d-derived states with a contribution from the Al 3p states. Above E_F, i.e. in the conduction band region, mainly the V 3d states contribute.

We have also calculated the coefficient of electronic specific heat γ for all these compounds (table 1) from our DOS value at E_F, $N(E_F)$, using the formula $\gamma = \pi^2 k_B^2 N(E_F)/3$. The γ value is the highest for V_3Al (45.4 mJ mol^{-1} K^{-2}) and the lowest for Fe_2VAl (0.45 mJ mol^{-1} K^{-2}). These values are in good agreement with available experimental and theoretical results for Fe_3Al [29], and with experimental results for Fe_2VAl [36]. The experimental value for Fe_3Al [29] differs from the calculated value by a factor of 1.09 only. This shows that the mass enhancement factor for this compound is very small. It is interesting to note that our $N(E_F)$ and γ values for Fe_2VAl, the compound with the 'pseudogap', are in very good agreement with the experimental value [36]. We recall that the reporting of a 0.1–0.2 eV gap at E_F in Fe_2VAl by experimental study [10] would mean necessarily no DOS at E_F. Thus, we conclude that the experimental studies of Fe_2VAl are indeed strongly dependent on sample preparation as proposed by Podgornykh *et al* [36]. They found that measurements of electronic specific heat of Fe_2VAl showed values which were very diverse and strongly dependent on the method of preparation, heat treatment or annealing of the sample. Some samples showed very low $N(E_F)$ (0.18 states/eV) as predicted by our first-principles calculations, whereas some others exhibited a larger value (4.8 states/eV) indicating heavy-fermionic-like behavior. To account for the larger value, they proposed that the lattice samples of paramagnetic Fe_2VAl contain a certain number of ferromagnetic clusters (defects) oscillating along the direction determined by crystallographic anisotropy energy. In addition, based on the thorough analysis of the temperature dependence of resistivity, Hall effect and photoemission data, Okamura *et al* [10] proposed that the Fermi level in Fe_2VAl may be shifted from the middle of the 'pseudogap' to the sharply rising portion of the valence band. Hence it would not behave as a low gap semiconductor and rather would be a semimetal; this supports our findings. Comparing our $N(E_F)$ and γ values for Fe_2VAl with experimental values (0.18 states/eV and 0.42 mJ mol^{-1} K^{-2}, respectively) for the samples regarded as defect-free, we find a very good agreement. Hence we conclude that our calculations are quite consistent.

For the optical conductivity (OC), we note that the experimental data is available only for Fe_3Al and Fe_2VAl. Hence we first discuss the results for these two compounds with respect to the experimental data [10]. Since there are sharp structures for energies <1 eV in experimental OC spectra of Fe_3Al, therefore it is essential to consider the intraband contribution to the optical conductivity. The OC spectra with Drude contribution (i.e. interband + intraband) are shown in figure 5 where we have also plotted the interband contribution alone (i.e. the conductivity without the Drude term) to bring out the effect of the intraband transitions. There is a significant intraband contribution to the conductivity below 1 eV in ferromagnetic Fe_3Al and the good agreement with experimental data in this low energy range may be credited to the intraband contribution. Interestingly, on the other hand, there is almost no difference on including the intraband transitions in the case of the nonmagnetic compound Fe_2VAl. This surprising result can be understood by examining the band structure of these compounds in the vicinity of E_F. The inset

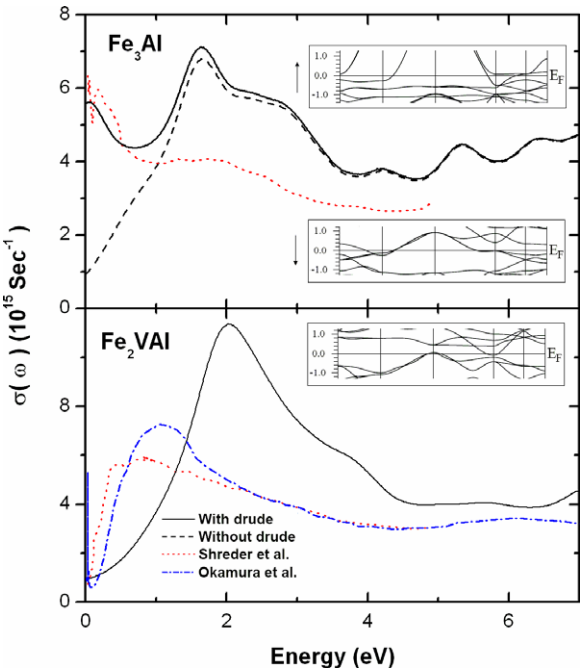

Figure 5. Calculated optical conductivity $\sigma(\omega)$ of $Fe_{3-x}V_xAl$ ($x = 0, 1$) compounds with their experimental counterparts. The inset shows the energy bands in the vicinity of the Fermi level, responsible for intraband transitions.

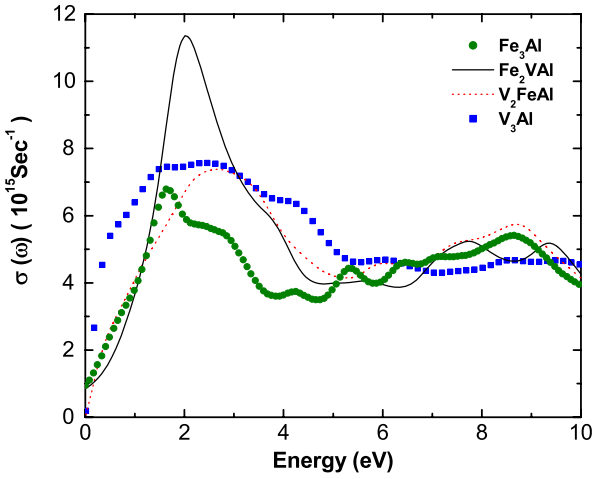

Figure 6. Comparison of calculated optical conductivity $\sigma(\omega)$ of $Fe_{3-x}V_xAl$ ($x = 0$–3) compounds.

in figure 5 showing this part of the band structure indicates that, for the bands intersecting the E_F in Fe_3Al, there are many occupied flat regions just below E_F with a significant amount of unoccupied states in the same band just above E_F. This facilitates intraband transitions in Fe_3Al. The situation, however, is entirely different for Fe_2VAl, the compound with the 'pseudogap', in which the bands intersecting E_F do not have either ample unoccupied regions or ample occupied regions in the vicinity of E_F (as is clear from the inset), making the intraband contribution totally insignificant. This results in an almost nonexistent intraband contribution in Fe_2VAl.

The qualitative behavior of theoretical and experimental OC curves is almost similar for Fe_3Al, though the calculations overestimate the OC beyond 1 eV. For Fe_2VAl, we find that the experimental data from Shreder *et al* [12] and Okamura *et al* [10] differ in the low energy region (<2 eV): however, the two overlap thereafter. This also indicates that the arrangement of bands near E_F or the presence of the 'pseudogap' in Fe_2VAl is strongly sample-dependent. Our results show a better agreement with the experimental data from Okamura *et al* [10] which is available for a larger energy range (up to 10 eV). Hence, we use this for comparison. We note that our results are able to reproduce the two peaks in experimental data. The calculated peak positions are, however, blueshifted by about 1 eV for the main peak and by ∼1.5 eV for the other. This behavior is similar to that of other half-metallic ferromagnets (e.g. CrO_2) where the frequencies (or energies) of the main spectral lines in OC plots, calculated within the DFT, are systematically overestimated by 10–20% [39]. The shoulder following the main peak in experimental data is also reproduced nicely by our calculations. The magnitude of $\sigma(\omega)$ is, however, overestimated, which may be attributed to the sensitive nature of the band structure near E_F. Further, the overestimation of the OC suggests that the calculated curves need a larger relaxation to be incorporated. However, on performing calculations with a stronger relaxation of ∼1 eV, we find that, although the agreement improves magnitude-wise, the structures are almost lost. In order to obtain a better agreement with experiment for OC spectra of Fe_2VAl, we repeated our calculations by choosing a stricter criterion and also by increasing further the number of k-points in the IBZ. However, there was no significant improvement with regards to the absorption peaks and other structures. This is due to the difference in the basic nature of the samples used for optical studies ([10] and [12]) as compared to those prepared and studied by Podgornykh *et al* [36], the latter (as already stated) giving a very good agreement with our first-principles results. However, fresh measurements on OC spectra of various samples of Fe_2VAl, particularly the kind prepared by Podgornykh *et al* [36], are welcome for a better comparison.

The highest peak at energy $E \sim 2$ eV, in both Fe_3Al and Fe_2VAl, is derived mainly from the transitions from V 4s and Al 3p states to unoccupied Fe 3d states. The transitions between 3d states of V and Fe across the 'pseudogap' also contribute to this prominent peak in the case of Fe_2VAl. The band structure and DOS curves clearly show why the main peak at ∼2 eV has a smaller magnitude in the case of Fe_3Al as compared to that for Fe_2VAl. The former has mainly the minority states responsible for this peak whereas, in Fe_2VAl, a good number of states are available on both sides of the 'pseudogap' to give a stronger peak. The large spread of empty states in both the compounds leads to the appearance of a more pronounced right shoulder following the main peak.

In figure 6, we compare the calculated optical conductivity of all the $Fe_{3-x}V_xAl$ compounds studied in this work. The intraband transitions have significant contributions for energies <1 eV in all these compounds except Fe_2VAl. The reason for the same has already been mentioned. Despite

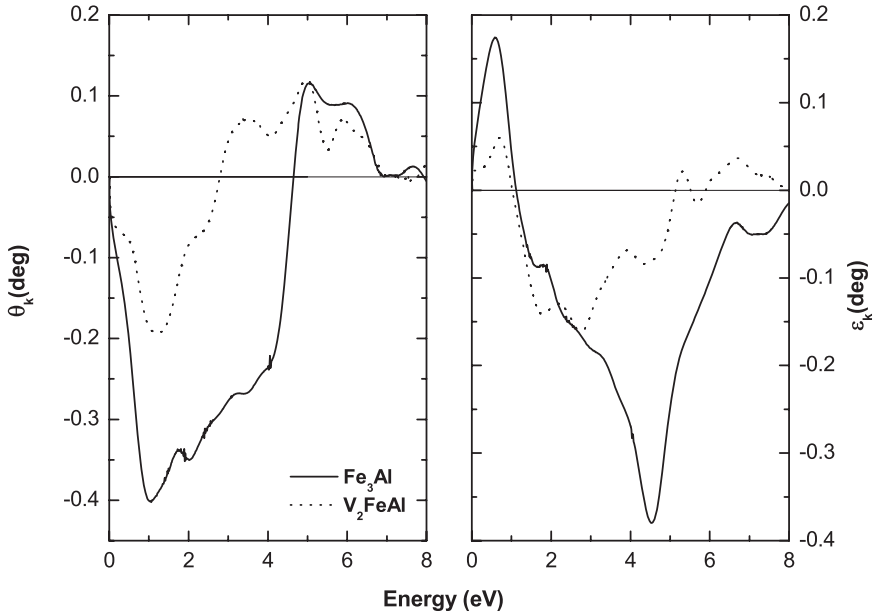

Figure 7. Polar Kerr rotation (θ_k) and ellipticity (ε_k) for Fe_3Al and V_2FeAl.

considerable differences between the band structures of the various compounds, their optical responses are fairly similar qualitatively. In most of the spectra, the optical absorption rises sharply and has a peak in the energy range 2–3 eV. The magnitude of this peak is the largest for Fe_2VAl in the series and is almost the same for the rest. It is due to larger overlapping of energy bands near E_F in these as compared to the case of Fe_2VAl. The OC spectra show structures and variations for energies up to 6 eV above which the behavior for magnetic Fe_3Al and V_2FeAl is quite similar while the curves become almost flat for NM Fe_2VAl and V_3Al. A close look at OC spectra reveals that V_3Al shows broadened structures near 2 eV whereas the other three compounds have relatively sharp peaks in this region. This difference is due to the different local environment in V_3Al (A15 structure) as compared to the other compounds (DO_3 and $L2_1$ structures).

We have also calculated the magneto-optical properties for the magnetic compounds Fe_3Al and V_2FeAl. The polar Kerr rotation and ellipticity for these compounds are shown in figure 7. Clearly, Kerr ellipticity and rotation are related: when the Kerr ellipticity crosses the zero line, a peak appears in the Kerr rotation spectra due to the Kramers–Kronig relations [40]. It is interesting to note that the theoretical ellipticity curve crosses and/or touches the zero axis a number of times; hence suggesting that the incident linearly polarized light, at these frequencies, would stay as linearly polarized only. In particular, there is the first magneto-optical resonance of $-0.4°$ at $E = 1$ eV in Fe_3Al and of $-0.19°$ at $E = 1.5$ eV in V_2FeAl. The other main peaks are located at 5 and 7 eV for Fe_3Al, whereas in V_2FeAl though we observe a number of small peaks in the energy range 3–6 eV but these are not of practical importance. The relatively large Kerr rotation in Fe_3Al is consistent with the larger magnetic moment of this compound.

5. Conclusions

In summary, we have performed first-principles density functional calculations to systematically investigate the structural and electronic properties of $Fe_{3-x}V_xAl$ compounds focusing on the $x = 0$–3 composition. Optimized lattice parameters, band structures, densities of states and optical conductivity spectra have been obtained. The calculated DOS at E_F is in good agreement with the experimental value, available only for Fe_3Al and Fe_2VAl. Our calculations predict and justify a large value of the coefficient of electronic specific heat for V_3Al, and a negligibly small value for Fe_2VAl. Also, our results support the findings by Podgornykh *et al* [36] that the properties of Fe_2VAl are strongly sample-preparation-dependent. We note that the magnetism is governed by the presence of Fe atoms in the bcc environment at (1/2 1/2 1/2) in $Fe_{3-x}V_xAl$ ($x = 0$–3). The site-resolved magnetic moments for Fe_3Al are in accordance with other theoretical calculations and experiments. This compound shows a relatively smaller magnetic moment at a lower lattice constant. The computed optical conductivity spectra reproduce the main features in the experimental spectra but systematically overestimate the positions of the main spectral peaks for both Fe_2VAl and Fe_3Al. The deviation in terms of magnitude is larger in Fe_2VAl which can be explained from the DOS of these materials in the neighborhood of E_F. In view of the strong dependence of properties of Fe_2VAl on the sample preparation method, it is desirable that fresh measurements on the optical conductivity of Fe_2VAl be made to help draw a more meaningful comparison. Our results show and explain why the intraband contribution to OC is important in Fe_3Al whereas for Fe_2VAl it is negligible. Various transitions responsible for structures in OC spectra are identified with the help of band structures. All the studied compounds show an intense peak in OC spectra in the energy range 2–3 eV and the OC spectra

are sensitive to radiation up to 5 eV only. Our study of the magneto-optical properties of the magnetic compounds Fe_3Al and V_2FeAl shows that Kerr rotation is larger in Fe_3Al than in V_2FeAl, consistent with the larger magnetic moment of the former. However, the maximum Kerr rotation of $-0.4°$ for Fe_3Al and of $-0.19°$ for V_2FeAl is not very appealing for magneto-optoelectronic applications.

Acknowledgment

The computation in this work was performed using the facilities provided by the Department of Physics, Indian Institute of Technology, Roorkee (Uttarakhand), India.

References

[1] Kato M, Nishino Y, Mizutani U and Asano S 2002 *J. Phys.: Condens. Matter* **12** 1769
[2] Ooiwa K and Endo K 1998 *J. Magn. Magn. Mater.* **177** 1443
[3] Guo G Y, Botton G A and Nishino Y 1998 *J. Phys.: Condens. Matter* **10** 19
[4] Singh D J and Mazin I I 1998 *Phys. Rev.* B **57** 14352
[5] Ruben W and Pickett W E 1998 *Phys. Rev.* B **58** 6855
[6] Bansil A, Kaprzyk S, Mijnarends P E and Tobola J 1999 *Phys. Rev.* B **60** 13396
[7] Burch T J, Raj K, Jena P, Budnick J I, Nichlescu V and Mair W B 1979 *Phys. Rev.* B **19** 2933
[8] Pickart S J and Nathans R 1961 *Phys. Rev.* **123** 1163
[9] Kumar M and Auluck S 2007 *Physica* B **390** 185
[10] Okamura H, Kawahara J, Nanba T, Kimura S, Soda K, Mizutani U, Nishino Y, Kato M, Shimoyama I, Miura H, Fukui K, Nakagawa K, Nakagawa H and Kinoshita T 2000 *Phys. Rev. Lett.* **84** 3674
[11] Wootan F 1972 *Optical Properties of Solid* (New York: Academic)
[12] Shreder E I, Kirillova M M, Makhnev A A and Dyakina V P 2002 *Phys. Met. Metallogr.* **93** 152
[13] Villars P and Calvert L D 1991 *Pearson's Handbook of Crystallographic Data for Intermetallic Phase* (Materials Park, OH: ASM)
[14] Watson R E and Weinert M 1998 *Phys. Rev.* B **58** 5981
[15] Kubo R 1957 *J. Phys. Soc. Japan* **12** 570
[16] Wang C S and Callaway J 1974 *Phys. Rev.* B **9** 4897
[17] Drude P 1900 *Z. Phys.* **1** 161
[18] Sommerfeld A and Bethe H 1933 *Handbuch der Physik* (Berlin: Springer)
[19] Kahn F J, Pershan P S and Remeika J P 1969 *Phys. Rev.* **186** 891
[20] Reim W and Schoenes J 1990 *Ferromagnetic Materials* vol 4, ed E P Wohlfarth and K H J Buschow (Amsterdam: North-Holland) chapter 5 p 493
[21] Blaha P, Schwarz K, Madsen G K H, Kvasnicka D and Luitz J 2001 *WIEN2k, An Augmented Plane Wave + Local Orbitals Program for Calculating Crystal Properties* Karlheinz Schwarz, Techn. Universitat Wien, Wien, Austria, ISBN 3-9501031-1-2
[22] Singh D J 1994 *Plane Waves, Peudopotential and the LAPW Method* (Boston: Kluwer-Academic)
[23] Wimmer E, Krakauer H, Weinert M and Freeman A J 1984 *Phys. Rev.* B **24** 864
[24] Weinert M, Wimmer E and Freeman A J 1982 *Phys. Rev.* B **26** 4571
[25] Perdew J P and Wang Y 1992 *Phys. Rev.* B **45** 13244
[26] Perdew J P, Burke K and Ernzerhof M 1996 *Phys. Rev. Lett.* **77** 3865
[27] Bennett H S and Stern E A 1965 *Phys. Rev.* **137** A448
[28] Kunes J, Novak P, Divis M and Oppeneer P M 2001 *Phys. Rev.* B **63** 205111
[29] Hsu L S, Wang Y K, Guo G Y, Soda K, Hayasaki M and Mizutani U 2002 *Phys. Rev.* B **66** 205203
[30] Xu B, Liu J and Yi L 2007 *Phys. Lett.* A **363** 312
[31] Klein B M, Boyer L L and Papaconstantopoulos D A 1978 *Phys. Rev.* B **18** 6411
[32] Nishino Y, Kato M, Asano S, Soda K, Hayasaki M and Mizutani U 1997 *Phys. Rev. Lett.* **79** 1909
[33] Guoy G Y, Bottonz G A and Nishinok Y 1998 *J. Phys.: Condens. Matter* **10** L119
[34] Wakiyama T 1972 *J. Phys. Soc. Japan* **32** 1222
[35] Bansil A, Kaprzyk S, Mijnarends P E and Tobola J 1999 *Phys. Rev.* B **60** 13396
[36] Podgornykh S M, Svyazhin A D, Shreder E I, Marchenkov V V and Dyakina V P 2007 *JETP* **105** 42
[37] Kumar M, Nautiyal T and Auluck S 2009 *J. Phys.: Condens. Matter* **21** 196003
[38] Ozolins V and Korling M 1993 *Phys. Rev.* B **48** 18304
[39] Mazin I I, Singh D J and Draxl-Ambrosch C 1999 *Phys. Rev.* B **59** 411
[40] Weng H, Kawazoe Y and Dong J 2006 *Phys. Rev.* B **74** 085205